Atmos. Meas. Tech. Discuss., 5, 2821–2855, 2012
www.atmos-meas-tech-discuss.net/5/2821/2012/
doi:10.5194/amtd-5-2821-2012

Atmospheric Measurement Techniques Discussions

Evaluation of continuous water vapor δD and δ^{18}O measurements by off-axis integrated cavity output spectroscopy

N. Kurita[1,2], **B. D. Newman**[1,*], **L. J. Araguas-Araguas**[1], **and P. Aggarwal**[1]

[1]International Atomic Energy Agency (IAEA), P.O. Box 100, Vienna, A1400, Austria
[2]Japan Agency for Marine-Earth Science and Technology, 2–15 Natsushima-cho, Yokosuka, 237-0061, Japan
[*]now at: Los Alamos National Laboratory, Losalamos, USA

Received: 21 March 2012 – Accepted: 3 April 2012 – Published: 16 April 2012

Correspondence to: N. Kurita (nkurita@jamstec.go.jp)

Published by Copernicus Publications on behalf of the European Geosciences Union.

Abstract

Recent commercially available laser spectroscopy systems enabled us to continuously and reliably measure the δD and δ^{18}O of atmospheric water vapor. The use of this new technology is becoming popular because of its advantages over the conventional approach based on cold trap collection. These advantages include much higher temporal resolution/continuous monitoring and the ability to make direct measurements of both isotopes in the field. Here, we evaluate the accuracy and precision of the laser based water vapor isotope instrument through a comparison of measurements with those found using the conventional cold trap method. A commercially available water vapor isotope analyzer (WVIA) with the vaporization system of a liquid water standard (Water Vapor Isotope Standard Source, WVISS) from Los Gatos Research (LGR) Inc. was used for this study. We found that the WVIA instrument can provide accurate results if: (1) correction is applied for time-dependent isotope drift, (2) normalization to the VSMOW/SLAP scale is implemented, and (3) the water vapor concentration dependence of the isotopic ratio is also corrected. In addition, since the isotopic value of water vapor generated by the WVISS is also dependent on the concentration of water vapor, this effect must be considered to determine the true water vapor concentration effect on the resulting isotope measurement.

To test our calibration procedure, continuous water vapor isotope measurements using both a laser instrument and a cold trap system were carried out at the IAEA Isotope Hydrology Laboratory in Vienna from August to December 2011. The calibrated isotopic values measured using the WVIA agree well with those obtained via the cold trap method. The standard deviation of the isotopic difference between both methods is about 1.4 ‰ for δD and 0.28 ‰ for δ^{18}O. This precision allowed us to obtain reliable values for *d*-excess. The day-to-day variation of *d*-excess measured by WVIA also agrees well with that found using the cold trap method. These results demonstrate that a coupled system, using commercially available WVIA and WVISS instruments can provide

continuous and accurate isotope data, with results achieved similar to those obtained using the conventional method, but with drastically improved temporal resolution.

1 Motivation

Global monitoring of oxygen and hydrogen isotope contents in precipitation has been carried out by the International Atomic Energy Agency (IAEA) in cooperation with the World Meteorological Organization (WMO) for more than 40 yr through the IAEA/WMO Global Network of Isotopes in Precipitation (GNIP). GNIP has led to a great deal of study of the temporal and spatial variations of environmental stable water isotopes (δ^{18}O and δD) and is widely used in various scientific disciplines, such as hydrology, climatology, ecology and biology (e.g., Araguas-Araguas et al., 2000; Hoffmann et al., 2000; Bowen et al., 2005). On the other hand, although water vapor is ubiquitous in the atmosphere, the availability of isotopic data on atmospheric water vapor is quite limited. One of the main reasons for this scarcity is that water vapor sampling presents more difficulties than precipitation sampling. Traditionally, atmospheric water vapor samples for isotope analysis were trapped in a cold bath filled with a cooling agent, such as liquid N_2 or dry ice/ethanol. Next, a collected water sample was extracted from the cold trap and analyzed using isotope ratio mass spectrometry (IRMS) or laser spectroscopy methods from the liquid water samples. Because incomplete trapping of water vapor results in isotope fractionation, self-designed trap system (Schoch-Fischer et al., 1984; Yakir and Wang, 1996; He and Smith, 1999; Uemura et al., 2008) have been developed to meet required trapping efficiency. In addition, extensive laboratory work is necessary to extract a vapor sample from a cold trap. More recently, alternative moisture trapping techniques have been reported, resulting in more sophisticated methods (Helliker et al., 2002; Han et al., 2006; Peters and Yakir, 2010). However, these methods are still labor intensive and require samples to be prepared in a laboratory.

A more recent alternative utilizes laser based instruments for water vapor isotope analysis. These instruments can directly measure atmospheric water vapor isotopes in

real-time with high temporal resolution without the time-consuming physical collection of condensed moisture (Griffith et al., 2006; Kerstel et al., 2006; Lee et al., 2005; Gupta et al., 2009; Sturm and Knohl, 2010). In addition, these instruments are of a reasonable size and power consumption is low, allowing the application of this technique to in-situ measurements (Griffith et al., 2006; Kerstel et al., 2006; Lee et al., 2005; Gupta et al., 2009; Sturm and Knohl, 2010). Notably, Lee et al. (2006) have reported continuous δD water vapor records for New England, USA, for a period of one year, using a tunable diode laser (TDL) spectroscopy system. However, because of instrumental nonlinearity, drifting signal, dependence on water vapor concentration, temperature sensitivity, and pressure variations in the absorption cell, regular and frequent calibration with a water vapor standard of known isotope content is required for long-term field observations. In addition, a required water vapor isotope standard of known isotopic content is not commercially available. Therefore, custom-made vaporizer systems, which can provide a frequent supply of water vapor of known isotope content to a laser instrument, had to be developed before such an instrument could be deployed in the field (Lee et al., 2005; Iannone et al., 2009; Schmidt et al., 2010; Sturm and Knohl, 2010). This represented a major limitation for the widespread use of this technique. However, a recently developed robust vaporizer system, coupled with the laser instrument, has become commercially available. Tremoy et al. (2011) have tested the performance of the calibration system (Standard Delivery Module, SDM) produced by Picarro, Inc. coupled with their laser instrument (Wavelength- Scanned Cavity Ring-Down Spectroscopy, WS-CRDS).

In this study, we use another commercially available instrument based on off-axis integrated cavity output spectroscopy, manufactured by Los Gatos Research, Inc. (LGR) (Water Vapor Isotope Analyzer, WVIA) coupled with an accessory device for the vaporization of a liquid water standard (Water Vapor Isotope Standard Source, WVISS). The WVISS is programmable from the WVIA and thus this coupled system is capable of automatically conducting a calibration routine at specific intervals. A detailed assessment of the WVIA has already been undertaken in previous studies (Wang et al., 2009; Sturm and Knohl, 2010; Rambo et al., 2011). Sturm and Knohl (2010) have

reported a strong concentration dependence and temperature sensitivity of the WVIA. Rambo et al. (2011) have used same coupled system with the WVISS and proposed a routine calibration procedure to correct for both concentration dependence and temperature sensitivity. These studies have highlighted the usefulness of this system to the field monitoring, however the long-term stability of an isotope monitoring test for atmospheric water vapor has not been reported yet. In particular, the performance and reliability of the calibration system (WVISS) must be stringently examined before it can be applied in field conditions. Here, we detail the results of extensive laboratory experiments to develop a calibration procedure for routine field application. Then, the calibration procedure developed from the laboratory experiment was evaluated through a long-term monitoring program of water vapor isotopes, using both the laser instrument and the conventional cryogenic moisture trapping method.

2 Experimental

2.1 Laser spectroscopy system

The laser spectroscopy system used to measure water vapor isotopes (δ^{18}O and δD) was the model DLT-100 water vapor isotope analyzer (WVIA, LGR Inc., Mountain View, CA, USA) manufactured in June 2009 (model 908-0004). The operating software was updated to the latest version in May 2011. This analyzer is based on an off-axis integrated cavity output spectroscopy system (OA-ICOS) using a semiconductor diode laser with a wavelength of around 1.39 µm (e.g., Bear et al., 2002). Here we describe the OA-ICOS measurement technique briefly. In OA-ICOS, the laser beam is directed off-axis with respect to the optical cavity. The laser wavelength is swept through the selected absorption line of each species (H_2O, HDO, and $H_2^{18}O$) and the transmitted laser intensity through a cavity is recorded. In addition, to determine effective optical path length in the cavity at each wavelength, ring down-time measurement is made by rapidly switching off the laser diode, which is measuring decay of the light intensity

over time. The typical ring-down time is around 10 s at 10 000 ppm H_2O concentration and it corresponds to the effective path length of 3 km in a 0.59 m-long cell. This path length is more than 10 times longer than that of the multi-pass cell and results in a high signal to noise ratio for isotope measurement. The mixing ratio χ of each water isotope species is determined through integration of the absorption spectrum as follows:

$$\chi_x = \frac{1}{S_x L_{\text{eff}} P} \int \ln\left(\frac{I_o}{I_\nu}\right) \mathrm{d}\nu$$

where I_ν is the transmitted laser intensity at wavelength ν, I_o is the initial intensity, P is gas pressure in the cell, S is absorption line strength, L_{eff} is effective optical path length. The subscript x represents each water isotope species. Calculated mixing ratios of water isotopologues are converted into a δ value with respect to the international standard Vienna Standard Mean Ocean Water (V-SMOW) (Coplen, 1996).

$$\delta = \left(\frac{R}{R_{\text{VSMOW}}} - 1\right) * 1000$$

where R is the atomic ratio, D/H or $^{18}O/^{16}O$, respectively.

2.2 Experimental setup for water vapor isotope measurement

A sample of air is introduced into an absorption cell (optical cavity) of the WVIA via an external pump (KNF, N920AP.29.18) downstream of the instrument at a constant flow rate of 0.5 l min^{-1}. The pressure in the absorption cell is controlled at 37 ± 0.007 hPa by a pressure controller and temperature is maintained at 49 °C to avoid the condensation of water vapor from ambient air in the cell. The data output frequency for water isotopologue measurements is 1 Hz.

To introduce water vapor standards into the WVIA, we used an LGR Water Vapor Standard Source (WVISS) device, manufactured in April 2010 (see Fig. 1a). It consists of a two-stage air dryer unit and a heated evaporation jar (1 l) for accepting water

from a 0.5 l container via a nebulizer (part no. 800-1-005-01-00; Savillex Ltd., Eden Prairie, MN, USA). Compressed room air is passed through a desiccant dryer (part no. MDH5-FLE-S37, Twin tower engineering, Broomfield, CU, USA) and a column of granular Drierite (size 8–20 mesh), providing dry air into the system (H_2O concentration <10 ppm). The compressed dry air stream from the drying unit is then split into two lines: one goes into the evaporation jar and the other supplies air to the nebulizer. The nebulizer aspirates liquid water from a water reservoir at a rate of 50 µl min^{-1} and injects tiny water droplets into the evaporation jar. The jar is heated to about 80 °C so that droplets are immediately evaporated; the resulting vapor should have the same isotopic composition as that of the source water. The humidity of the output air can be varied from 2500 to 25 000 ppm by adjusting the dry air mixing ratio in the evaporation jar. The flow of dry air is controlled by a mass flow controller (part no. FMA5420, OMEGA Engineering, Stamford, CT, USA, 0–5 l min^{-1}).

The output tubing from the jar is connected to a T-shape splitter via 3/8 inch (9.52 mm) Teflon tubing. One outlet constitutes an exhaust to room air, whereas the other outlet is directed to the analyzer through a 3-way valve, which controls airflow by switching between the ambient air inlet and WVISS-generated standard gas. The WVISS-generated standard gas is drawn by an external pump downstream of the analyzer (see above). The tubing joining the WVISS and the analyzer is made of 1/4 inch (6.35 mm) Teflon tubing (with a length of around 1 m). The dilution rate with dry air and valve operation is controlled by the WVIA. Raw data from the analyzer is stored on both the internal hard disk and the external computer, and is transferred via ethernet cable. Calibration is undertaken as a post-processing step using the external computer system.

2.3 Performance test of the WVISS

To test the assumption that no fractionation occurs in the WVISS, air generated in the unit was physically collected using a cold trap (see Fig. 1a). A water reservoir was filled with an in-house laboratory water standard (δD = −78 ‰ and δ^{18}O = −11.3 ‰), then

the WVISS was run continuously during vapor trapping (2–6 h) to obtain a sufficient amount of water for isotope analysis. WVISS air exhaust was drawn by an external pump at a flow rate of 1.5 l min^{-1},then water vapor was collected with a glass trap submerged into a dry-ice/isopropanol mixture at −78 °C. This experiment was repeated more than 10 times at 6 levels of water vapor concentration (3000 ppm, 4000 ppm, 5500 ppm, 6000 ppm, 8000 ppm, 10 000 ppm). In this study, we used a custom manufactured glass trap for vapor collection. This trap has been used for water vapor sample collection in various field projects (Kurita and Yamada, 2007; Kurita, 2011; Kurita et al., 2011). Along with this, we undertook a trapping test using the WVISS/WVIA system before starting the laboratory experiment. A glass trap was inserted between WVISS and WVIA and output humidity from a cold trap was monitored by the WVIA. This pretest confirmed complete trapping of water vapor because the reported humidity from the WVIA is less than 10 ppm during such a trapping period.

The collected amount of water was less than 1.5 g. After sample collection, water in the trap was subsequently thawed and poured into a 9-ml glass vial. Isotopic analysis of the collected water was undertaken at the IAEA Isotope Hydrology Laboratory using IRMS (Delta plus, Thermo Scientific, Bremen, Germany) with a locally developed equilibration device and through cavity ring-down spectroscopy isotopic water analysis (model L1102-i; Picarro Inc., Sunnyvale, CA, USA) with a CTC Analytics autosampler (model HTC-PAL; Leap Technologies, Carrboro, NC, USA). Measurement precision, including internal and external variation, is better than ±0.15 ‰ for δ^{18}O and ±2 ‰ for δD.

During vapor trapping, the WVISS generated vapor was introduced into the WVIA for 10 min in every hour. To comparison with the values of water vapor samples collected by cold trap method, the time-averaged isotopic values of WVIA measurements were calculated from the last 5 min of each 10 min continuous measurement run every hour.

2.4 Accuracy and precision of the WVIA measurement

Isotope measurements of nine in-house water standards with different $\delta^{18}O$ and δD contents (Table 1) were performed to help determine a routine calibration procedure for the coupled WVIA and WVISS system. The water standards ranged in isotope values from −397.9 to −0.1 ‰ for δD and from −50.87 to −0.08 ‰ for $\delta^{18}O$. Each water standard was stored in a 9-ml glass vial. The nebulizer feed tube was inserted into a vial of standard, and the mixing ratio of the WVISS-generated vapor was set to 10 000 ppm. Vapor was continuously introduced into the WVIA and the isotope data for the last 10 min of the 20 min measuring periods was averaged. After a 20 min measurement period, the water bottle with the isotope standard was replaced. To reduce memory effects from residual water, water in the tubing was flushed away with dry air before the tube was inserted into a next standard. As described in Sturm and Knohl (2010), the WVIA response time is short, thus we did not observe any memory effect in the isotopic data during the final 10 min period, even though the most negative water standard (STD10) was measured just after the least negative water standard (STD11). Measurements of the nine water standards were performed during the same day (the measurement sequence was random) and the experiment was repeated more than 15 times.

2.5 Ambient air analysis

To evaluate the overall calibration procedure, we measured water vapor isotopes in ambient air using the WVIA-WVISS coupled system from August to December 2011. A sampling tube for outdoor air (5 m length of BEV-A-Line V tubing, 1/4 inch O.D.) was connected to a 3-way valve attached to the WVISS (see Fig. 1b). The outdoor air tube was used to sample the ambient water vapor present in Vienna, Austria outside our laboratory (tubing was routed through a window). A 1.0 µm filter with PTFE membrane (part no. 10463523, Whatman, Dassel, German) was placed where the tube enters the WVISS. Air was drawn via the WVIA external pump at a flow rate of 0.5 l min^{-1}. Every

50 min, the 3-way valve automatically switched from ambient/outdoor inlet to WVISS standard air, whereupon standard air with a H_2O concentration of 10 000 ppm was introduced to the WVIA for 10 min. After finishing the reference gas measurement, the valve switches back and ambient air sampling is resumed.

Atmospheric water vapor sampling using the cold trap method was also carried out to evaluate the validity of laser based water isotope measurements. Air sampling tubing (10 m length of PVC tubing, 14 mm O.D.) with an inlet at the same location as the WVISS ambient inlet was attached to a glass trap, which is the same as that used in the WVISS performance test (Fig. 1b). Air was drawn at a rate of 1.5 l min^{-1} through the trap immersed into a dry-ice/isopropanol bath for 6 to 15 h. The amount of water vapor trapped ranged from 1.6 to 13.2 g. We collected 154 samples from August to December 2011. The isotopic analysis of these samples was carried out using the procedure described above.

3 Results and discussion

3.1 Performance test of the WVISS

The mean isotopic values and the statistical distribution of the WVISS-generated air collected by cold trap, at several water vapor concentrations are shown in Fig. 2. There was a large spread in isotopic values greater than analytical uncertainty arising from water isotope measurement at each vapor concentration. To examine whether a large spread in isotopic values in WVISS-generated air is related to WVISS vapor production, the values of water vapor samples using the cold trap (δ_{TRAP}) technique are compared with WVIA-reported raw isotopic values (δ_{WVIA}) in Fig. 3. For δD, the spread of values from the cold trap samples is almost twice as big as that of the WVIA reported values. The variation in δD_{WVIA} values is less than ±2 ‰ from the mean value. The δD_{TRAP} values include analytical error, which take place during liquid water isotope measurement (around 2 ‰). In addition, decanting small amounts of trap water (less than 1.5 g) into

vials leads to additional scatter. The variation in δD_{WVIA} is similar or less than the analytical uncertainty of cold trap samples. This uncertainty may result in a large spread and thus data points plot under a 1:1 line. However, there is a positive correlation between δD_{WVIA} and δD_{TRAP} ($R = 0.369$) and a similar feature that the δD_{WVIA} values at 3000 ppm showed slightly enriched values, similar to the δD_{TRAP} (see purple dots in Fig. 3a). Although the amplitude of a spread may be overestimated due to analytical uncertainty of cold trapped samples, the variation of δD_{TRAP} values may reflect some isotopic shift in WVISS-generated air.

For $\delta^{18}O$, the relationship between $\delta^{18}O_{WVIA}$ and $\delta^{18}O_{TRAP}$ is scattered across the entire water vapor concentration range (3000 to 10 000 ppm) because of the time-dependent isotope variation (see next section). However, a linear correlation between $\delta^{18}O_{WVIA}$ and $\delta^{18}O_{TRAP}$ was observed in the measurements at 10 000 ppm when the time-dependent isotopic variation was small. The points at 10 000 ppm measured between 27–29 November 2011 (red circles) are clearly distributed along a 1:1 line and the spread is significantly larger than the analytical uncertainty (0.15 ‰) (Fig. 3b). This large spread at 10 000 ppm probably reflects isotopic changes in WVISS-generated air. This suggests that a large spread in $\delta^{18}O$ values of WVISS-generated air at each concentration may be related to WVISS vapor production. The average standard deviation in the range of 3000 to 10 000 ppm is about 0.25 ‰ for $\delta^{18}O$. In addition to a large spread in isotopic values, Fig. 2 shows that the mean isotopic value of WVISS-generated air varied in response to changing water vapor concentration. Measured $\delta^{18}O$ at higher concentrations (6000 to 10 000 ppm) is higher than the known value, and at lower water vapor concentrations (3000 to 5500 ppm), $\delta^{18}O$ values tend to be more negative than for higher concentrations. The mean value shifts from −11.1 ‰ at higher concentrations to −11.4 ‰ at lower concentrations. The difference between them is statistically significant ($p < 0.05$). On the other hand, δD data do not suggest the same behavior. A positive bias is observed at all concentrations. There is also no systematic difference in the isotopic contents of water vapor for concentrations ranging from 3000 to 10 000 ppm.

The humidity in WVISS output air is controlled through adjusting the dry air mixing ratio in the evaporation jar. To decrease the concentration from 10 000 ppm to 5000 ppm, the flow rate of air is increased from 1 l min^{-1} to 2.5 l min^{-1}. This means that turnover time in the jar becomes shorter from 1 min at 10 000 ppm to 0.4 min at 5000 ppm. If this time is not enough for complete evaporation from injected water drops, it will result in isotopic fractionation. Inefficient evaporation would tend to cause more negative oxygen isotope values than the source value. The gradual decrease in $\delta^{18}O$ values with decreasing concentration is consistent with inefficient evaporation. For δD the isotopic change due to this effect is relatively small, thus concentration dependence may be masked by analytical uncertainty. The tendency toward water vapor concentration dependence is consistent with the inefficient evaporation effect, however this effect cannot explain the positive bias of δD data at all concentrations and $\delta^{18}O$ data at relatively high concentrations (6000 to 10 000 ppm). This suggests that when the inefficient evaporation effect is ruled out, other effects may change the isotopic values of WVISS generated air. However, it is not essential to identify the source of uncertainty because the isotopic value of WVISS generated air is highly reproducible.

3.2 Accuracy and precision of the WVIA measurement

3.2.1 Long-term stability

The long-term stability of the WVIA was evaluated via repeated measurements of a water standard over a period of four months. The uncalibrated hourly measurement time series of a water standard ($\delta D = -78$ ‰ and $\delta^{18}O = -11.3$ ‰) at a constant concentration (10 000 ppm) is shown in Fig. 4. Each plot represents the last 5 min average value of a 10 min measurement. Measured isotopic values range from −77 ‰ to −82 ‰ for δD and from −8.0 ‰ to −12.5 ‰ for $\delta^{18}O$. The spread in $\delta^{18}O$ is three times larger than the difference between the maximum and minimum of WVISS-generated air at the same concentration (Fig. 2), indicating the variation stems mainly from the WVIA. Because an analyzer was installed in an air-conditioned laboratory, the observed large

isotopic variation is too large to be explained by temperature variations (Sturm and Knohl, 2010). It is not clear yet what is causing this large $\delta^{18}O$ variation, however it is clear that the system does have significant non-linear drift. Thus, frequent measurement of a water standard is crucial to correct for time-dependent isotope variation.

Next, we examined the similarity between the time-dependent variability in water standards with different isotopic values. The temporal variations in δD and $\delta^{18}O$ of the six water standards (see Table 1) are shown in Fig. 5. The data are represented as a normalized anomaly from the long-term mean value. The temporal trends of each standard water matched each other well for both isotopes, and they do not depend on the isotopic content of water. Thus, repeated measurements of a single reference water sample should be enough to remove time-dependent drift. To move the run-to-run variability, the WVIA-reported isotopic value of the water standard was converted to the VSMOW scale using a water standard (STD-11, see Table 1).

$$\delta_{\mathrm{WVIA}} = \left(\frac{\delta_{\mathrm{sample/raw}} - 1}{\delta_{\mathrm{std11/raw}} - 1} (\delta_{\mathrm{std11/VSMOW}} - 1) - 1 \right) \times 1000$$

where $\delta_{\mathrm{sample/raw}}$ and $\delta_{\mathrm{STD11/raw}}$ are the raw δD or $\delta^{18}O$ values of the sample and STD-11, respectively, and $\delta_{\mathrm{STD11/VSMOW}}$ is the VSMOW scale value determined by IRMS measurements.

3.2.2 Linearity

To test the linearity of the WVIA–WVISS coupled system, the WVIA-measured isotopic values of several water standards were compared with those obtained via IRMS measurements. The differences between values from the WVISS/WVIA and known values of each standard are shown in Fig. 6. For δD, except STDX3 ($\delta D = -332.7$‰), the calculated VSMOW scale value of each water standard agreed well with the known value. However, the WVISS/WVIA-$\delta^{18}O$ values significantly underestimated the true values, and the amplitude of this underestimation decreased linearly with increasing δ values.

A two-point calibration method was applied to normalize WVIA-reported data (δ_{WVIA}) to the international VSMOW/SLAP scale. The calibration line was determined from two different water standards, one which has more negative isotope contents (STD10) and another with more enriched isotopic values (STD11). The averaged lines obtained during the laboratory test are as follows:

$$\delta D_{\mathrm{IRMS}} = (1.001 \pm 0.003)\delta D_{\mathrm{WVIA}} - 0.85 \pm 1.03 \quad (1)$$

$$\delta O_{\mathrm{IRMS}} = (0.946 \pm 0.005)\delta O_{\mathrm{WVIA}} - 0.96 \pm 0.89 \quad (2)$$

The linear relationship between IRMS and WVIA measurements has already been reported in Sturm and Knohl (2010), however the slope for both isotopes are substantially different in this study. This finding suggests that linearity calibrations will likely be instrument specific. During the period of this laboratory test, the calibration line was determined every day and then applied for normalization to the VSMOW/SLAP scale. The results of the water standards measurements are summarized in Table 1 (Fig. 6 for $\delta^{18}O$). The isotopic difference between known and measured values is less than 1.5‰ for δD and 0.2‰ for $\delta^{18}O$. Thus, the corrected WVIA values agree well with known values within analytical error. In summary, obtaining accurate isotope data from WVISS/WVIA systems will require, at a minimum, correcting for time-dependent isotopic drift using a frequently repeated reference standard, and normalization of the drift corrected data to the VSMOW/SLAP scale using a two standard approach.

3.2.3 Concentration dependence

Previous studies have reported water vapor concentration dependence of δ values, and highlighted this factor as the primary source of analytical uncertainty (Sturm and Knohl, 2010; Rambo et al., 2011). Through the WVISS performance test a clear concentration dependence for $\delta^{18}O$ arising from the calibration system was uncovered, however this effect has not been fully considered in previous studies. The water vapor concentration effect, determined from raw WVIA isotopic values through the measurement of WVISS-generated air, together with the isotopic changes in WVISS-generated

air collected by cold trap are shown in Fig. 7. The responses to changes in water vapor concentration are shown as differences in isotope values from those measured at 10 000 ppm. Regarding δ^{18}O there is a increasing trend in δ^{18}O values with decreasing water vapor concentration for the WVISS/WVIA system that is a nearly linear match to that of WVISS-generated air up to a water vapor concentration of 6500 ppm. However, in the lower range of the concentration (lower than 6500 ppm), the δ^{18}O values of WVISS-generated air decreased inversely with water vapor concentration. These findings suggest that concentration dependence determined by WVIA–WVISS measurements is underestimated for low water vapor concentration. The corrected concentration effect arising from WVIA measurements was determined through subtraction of isotopic changes in WVISS-generated air. These results show that there is no effect in the concentration range of 6500 to 10 000 ppm and it gradually increases in the concentration range of 6500 to 4500 ppm. The δ^{18}O values at 3000 ppm were similar to those found at 4500 ppm. This non-linearity effect for δ^{18}O appears to be similar to that found by Sturm and Knohl (2010), although the amplitude of isotopic variations is smaller.

For δD, WVIA-reported raw isotopic values slightly increase with decreasing water vapor concentration from 10 000 ppm to 3000 ppm (not shown); this tendency is consistent with the result of cold trap samples (Fig. 2). However the spread of values from cold trap samples is larger than that of the WVIA reported values in the whole concentration range (Fig. 3) and thus we cannot conclude that this water vapor concentration dependency is related to WVISS vapor production. Because the amplitude of this shift is small (1 ‰ from 10 000 ppm to 3000 ppm), we do not consider the concentration dependence in this study. The amplitude is quite small compared to that reported by Sturm and Knohl (2010). The concentration effect results likely from the spectral fitting procedures used, including the removal of interferences in the WVIA. The spectral fitting procedure of our instrument was updated in May 2011 and the upgraded instrument may be less sensitive to the water vapor concentration effect.

3.3 Ambient air analysis

3.3.1 Calibration procedure

The calibration procedure developed from laboratory experiments was applied to the continuous measurement of water vapor isotopes. First, the WVIA-reported raw isotopic values were converted using the reference standard values to correct time-dependent isotopic drift. In the laboratory test, the reference standard was measured just once a day, however more frequent measurement of the reference is recommended for continuous measurement under routine conditions (see Fig. 4). For the measurements of outdoor air, the reference gas (which is set to a water vapor concentration of 10 000 ppm) was measured every hour for 10 min. The isotopic contents of the source water used as a reference were determined by IRMS measurement (δD = −79 ‰ and δ^{18}O = −11.3 ‰). The hourly reference data was interpolated to 10 min steps and the data at measuring time was used for reference scale conversion. For δ^{18}O, because humidity bias cannot be ignored, the observed non-linear function was applied to time-interpolated reference data and the corresponding reference value δ_{ref} at the concentration measured in ambient air was calculated as:

$$\delta \mathrm{D}_{\mathrm{ref}} = \left(\frac{(\mathrm{D}/\mathrm{H})_{\mathrm{raw}}}{(\mathrm{D}/\mathrm{H})_{\mathrm{ref}}} - 1 \right) \times 1000$$

$$\delta \mathrm{O}_{\mathrm{ref}} = \left(\frac{(^{18}\mathrm{O}/^{16}\mathrm{O})_{\mathrm{raw}}}{f(\mathrm{H_2O})(^{18}\mathrm{O}/^{16}\mathrm{O})_{\mathrm{ref}}} - 1 \right) \times 1000$$

where $\mathrm{D/H_{raw}}$ ($^{18}\mathrm{O}/^{16}\mathrm{O_{raw}}$) and $\mathrm{D/H_{ref}}$ ($^{18}\mathrm{O}/^{16}\mathrm{O_{ref}}$) are the WVIA-reported isotopic ratios of ambient air and water vapor reference generated by the WVISS. The $f(\mathrm{H_2O})$ represents a calibration function for the concentration effect shown in Fig. 7 (green line). As described in the previous section, we applied this function when the water vapor concentration of ambient air dropped lower than 6500 ppm, otherwise $f(\mathrm{H_2O}) = 1$.

Next, the reference scale value was converted to the VSMOW scale value and then normalized to the VSMOW/SLAP scale value using Eqs. (1) and (2). The measurement of multiple water standards was not performed during the measurement of ambient air, thus the long-term mean slope and intercept for δD and δ^{18}O value obtained from the laboratory test was used. The possible error in isotopic measurements when applying a constant slope and intercept was evaluated through a comparison with the results described in Sect. 3.3. Without daily calibration, the standard deviation of water standards increased a little, ranging from 0.79 to 1.32 ‰ for δD and from 0.19 to 0.39 ‰ for δ^{18}O. However, this error is relatively small compared to that arising from the uncertainty of the humidity bias correction.

3.3.2 Field data evaluation

To further test our calibration procedure, corrected WVIA data was compared with the results of cryogenic vapor collection/IRMS measurement. The continuous measurement of atmospheric vapor based on a laser instrument and ambient air sampling using the cold trap method was carried out from August to December 2011. During this period, more than 150 water vapor samples were collected using the cold trap method with water vapor concentrations ranging from 3000 to 15 000 ppm.

Even though several sources of uncertainty contribute to the degraded accuracy of water vapor isotope measurements using the WVIA, the primary source of uncertainty may be associated with non-linear dependency on the humidity bias correction. Because this function includes the uncertainties arising from both the WVIA and the WVISS (Fig. 7), the robustness of this function should be tested before applying it to field data. In Fig. 8a, the non-linear function was compared with the humidity bias obtained from ambient air measurement. For this comparison, we used WVIA data without correcting the water vapor concentration effect; these were integrated over time during vapor trapping. Although the data points are widely scattered in the low concentration range ($\sigma > 0.35$ ‰ at 4500 ppm, whereas $\sigma < 0.30$ ‰ between 6500 and 15 000 ppm),

a clear negative effect of water vapor concentration on δ^{18}O contents is seen in the field data. In addition, this humidity bias is in very good agreement with the calibration curve obtained from the laboratory experiment. Thus, applying the calibration function leads to a decrease in systematic offset depending on concentration (Fig. 8b). This finding emphasizes that the non-linear function reasonably represents concentration dependence arising from the WVIA. For δD, the concentration effect was not clearly seen in the field data, although the points are more scattered towards the region of decreasing water vapor concentration (Fig. 9).

Over the observation period, the δ^{18}O (δD) values observed from samples collected by the cold trap method varied widely from −27.1 ‰ (−199 ‰) to −13.1 ‰ (−94 ‰), and these large temporal changes were also successfully reflected by the WVIA values which in fact reveal even greater temporal dynamics than were possible to measure using the trapping approach (not shown). In addition, the time-series of the d-excess parameter ($d = \delta\mathrm{D} - 8 \times \delta^{18}\mathrm{O}$), defined by Dansgaard (1964) show reasonable consistency between the cold trap and WVIA analysis over a large range ($5 \sim 25$). The similarity between trap based values and WVIA based values is strong evidence that high quality high temporal resolution data can be obtained over a wide range of isotope values and humidity conditions with the WVISS/WVIA system. To further evaluate the accuracy and precision of δD and δ^{18}O measured with the WVIA, we calculated the time-averaged isotopic values during vapor trapping and then subtracted from the cold trap values for the same sampling periods (Fig. 10). The plots are scattered randomly in the range of −0.65 to 0.77 ‰ for δ^{18}O and from −3.8 to 2.9 ‰ for δD, and there is no offset. The mean value of the deviations of the 154 samples is 0.06 ± 0.28 ‰ for δ^{18}O and -0.3 ± 1.4 ‰ for δD, respectively. Thus, although there is substantial scatter the mean values for both isotopes are close to zero suggesting that our developed calibration procedure can provide accurate isotope data, similar to the conventional method. The relatively large random error may result from the several sources of uncertainty. As discussed earlier, there are uncertainties related to how WVIA/WVISS data were corrected and calibrated. More frequent linearity calibration may help to

reducing the random error. Regarding $\delta^{18}O$ the uncertainty of the isotopic value of WVISS-generated air is 0.25 ‰ and may contribute to random error. Further development of the calibration system may play a key role in reducing this random error. Finally, we evaluated the *d*-excess values by comparing the *d*-excess measured by the WVIA with that from the cold trap method (Fig. 11). Most data plot along the 1:1 line which indicates that our calibration procedure can provide *d*-excess data that are consistent with the conventional trap approach.

4 Summary and conclusions

Water vapor stable isotope measurements based on a commercially available laser instrument (WVIA) in conjunction with a calibration system (WVISS) was evaluated through laboratory experiments using several water standards. We found that WVIA instrument can provide accurate results if corrections are applied for: (1) temporal drift, (2) normalization to the VSMOW/SLAP scale, and (3) dependency of isotope results on water vapor concentration. Periodic VSMOW/SLAP normalization using two standards (linearization calibration) is especially important for $\delta^{18}O$ (and *d*-excess), because the slope of the calibration line between the WVIA-reported values and the IRMS value differs substantially from 1 in addition to drift correction for temporal variation using a frequently measured single reference standard as described by Rambo et al. (2011). Another remarkable finding of our study is that concentration dependence stems from the WVISS. The $\delta^{18}O$ values of vapor generated by the WVISS vary with time and depending on the output humidity concentration when vapor concentration becomes lower than 6500 ppm. In this study, we determined the "true" concentration effect stemming from the WVIA and then produced a new calibration procedure for WVIA measurement.

To test our calibration procedure and the instrumentation, continuous measurement of water vapor isotopes in ambient outdoor air was carried out from summer

to winter using the WVISS/WVIA system together with water vapor sampling using the conventional cold trap method. Despite water vapor concentrations that varied from 3000 to 15 000 ppm, the results from both methods agree well with throughout the entire observation period. The precision estimated from the comparison of both measurements is 0.28 ‰ for $\delta^{18}O$ and 1.4 ‰ for δD, respectively. These uncertainties allow calculation of representative *d*-excess values and to assess natural variability. The *d*-excess variations from the WVIA measurements reasonably match those obtained from cold trapped vapor. The fact that accurate *d*-excess values can be obtained is good confirnamtion of the overall performance of the instrument and calibration approach.

In summary, accurate water vapor isotope data, with results comparable to those achieved using conventional methods, can be obtained from commercially available systems with high time resolution. This suggests that isotopes in water vapor can be measured without special operational skills. In addition, laser based instruments do not require the manual effort and hassles. Thus, the laser based technique has substantial potential to increase the availability of water vapor isotope data which can significantly advance scientific understanding related to the water cycle.

Acknowledgements. We would like to thank Liliana Pöltenstein and Michael van Duren for liquid water isotope analysis in our laboratory, Manfred Jaklitsh for his help in the laboratory test and ambient air sampling, and Maureen Macneill for editing the original text.

References

Araguas-Araguas, L., Froehlich, F., and Rozanski, K.: Deuterium and oxygen-18 isotope composition of precipitation and atmospheric moisture, Hydrol. Process., 14, 1341–1355, 2000. 2823

Bear, D., Paul, J., Gupta, M., and O'Keefe, A.: Sensitive absorption measurements in the near-infrared region using off-axis integrated-cavity-output-spectroscopy, Appl. Phys. B-Lasers O., 75, 261–265, 2002. 2825

Bowen, G. J., Wassenaar, L. I., and Hobson, K. A.: Global application of stable hydrogen and oxygen isotopes to wildlife forensics, Oecologia, 143, 337–348, 2005. 2823

Coplen, T. B.: New reporting of stable hydrogen, carbon, and oxygen isotopic abundances, Geochim. Cosmochim. Ac., 60, 3359–3360, 1996. 2826
Dansgaard, W.: Stable isotopes in precipitation, Tellus, 16, 436–468, 1964. 2838
Griffith, D. W. T., Jamie, I., Esler, M., Wilson, S. R., Parkes, S. D., Waring, C., and Bryant, G. W.: Real-time field measurements of stable isotopes in water and CO_2 by Fourier transform infrared spectroscopy, Isot. Environ. Healt. S., 42, 9–20, 2006. 2824
Gupta, P., Noone, D., Galewsky, J., Sweeney, C., and Vaughn, B. H.: Demonstration of high-precision continuous measurements of water vapor isotopologues in laboratory and remote field deployments using wavelength-scanned cavity ring-down spectroscopy (WS-CRDS) technology, Rapid Commun. Mass Sp., 23, 2534–2542, 2009. 2824
Han, L.-F., Gröning, M., Aggarwal, P., and Helliker, B. R.: Reliable determination of oxygen and hydrogen isotope ratios in atmospheric water vapor absorbed on 3A molecular sieve, Rapid Commun. Mass Sp., 20, 3612–3618, 2006. 2823
He, H. and Smith, R. B.: Stable isotope composition of water vapour in the atmospheric boundary layer above the forests of New England, J. Geophys. Res., 104, 11657–11673, 1999. 2823
Helliker, B. R., Roden, J. S., Cook, C., and Ehleringer, J. R.: A rapid and precise method for sampling and determining the oxygen isotope ratio of atmospheric water vapor, Rapid Commun. Mass Sp., 16, 929–932, 2002. 2823
Hoffmann, G., Jouzel, J., and Masson, V.: Stable water isotopes in atmospheric general circulation models, Hydol. Process., 14, 1385–1406, 2000. 2823
Iannone, R. Q., Romanini, D., Kassi, S., Maijer, H., and Kerstel, E. R. T.: A microdrop generator for the calibration of a water vapor isotope ratio spectrometer, J. Atmos. Ocean. Tech., 26, 1275–1288, 2009. 2824
Kerstel, E. R. T., Iannone, R. Q., Chenevier, M., Kassi, S., Jost, H. J., and Romanini, D.: A water isotope (^{2}H,^{17}O, and ^{18}O) spectrometer based on optical-feedback cavity enhanced absorption for in-situ airbone applications, Appl. Phys. B-Lasers O., 85, 397–406, 2006. 2824
Kurita, N.: Origin of Arctic water vapor during the ice-growing season, Geophys. Res. Lett., 38, L02709, doi:10.1029/2010GL046064, 2011. 2828
Kurita, N. and Yamada, H.: The role of local moisture recycling evaluated using stable isotope data from over the middle of the Tibetan Plateau during the monsoon season, J. Hydrometeorol., 9, 760–775, 2007. 2828

Kurita, N., Noone, D., Risi, C., Schmidt, G. A., Yamada, H., and Yoneyama, K.: Intraseasonal isotopic variation associated with the Madden-Julian Oscillation, J. Geophys. Res., 116, D24101, doi:10.1029/2010JD015209, 2011. 2828
Lee, X., Sargent, S., Smith, R., and Tanner, B.: In situ measurement of the water vapor ^{18}O/^{16}O isotope ratio for atmospheric and ecological applications, J. Atmos. Ocean. Tech., 22, 555–565, 2005. 2824
Lee, X., Smith, R., and Williams, J.: Water vapour ^{18}O/^{16}O isotope ratio in surface air in New England, USA, Tellus B, 58, 293–304, 2006. 2824
Peters, L. I. and Yakir, D.: A rapid method for the sampling of atmospheric water vapour for isotopic analysis, Rapid Commun. Mass Sp., 24, 103–108, 2010. 2823
Rambo, J., Lai, C.-T., Farlin, J., Schroeder, M., and Bible, K.: On-site calibration for high precision measurements of water vapor isotope ratios using off-axis cavity-enhanced absorption spectroscopy, J. Atmos. Ocean. Tech., 28, 1448–1457, 2011. 2824, 2825, 2834, 2839
Schmidt, M., Maseyk, K., Lett, C., Biron, P., Richard, P., Bariac, T., and Seibt, U.: Concentration effects on laser-based δ^{18}O and δ^2H measurements and implications for the calibration of vapour measurements with liquid standards, Rapid Commun. Mass Sp., 24, 3553–3561, 2010. 2824
Schoch-Fischer, H., Rozanski, K., Jacob, H., Sonntag, C., Jouzel, J., Östlund, G., and Geyh, M.: Hydrometeorological factors controlling the time variation of D,^{18}O and ^{3}H in atmospheric water vapour and precipitation in the northern westwind belt, in: Isotope Hydrology 1983, 3–30, IAEA-publication, Vienna, Austria, 1984. 2823
Sturm, P. and Knohl, A.: Water vapor δ^2H and δ^{18}O measurements using off-axis integrated cavity output spectroscopy, Atmos. Meas. Tech., 3, 67–77, doi:10.5194/amt-3-67-2010, 2010. 2824, 2829, 2833, 2834, 2835
Tremoy, G., Vimeux, F., Cattani, O., Mayaki, S., Souley, I., and Favreau, G.: Measurements of water vapor isotope ratios with wavelength-scanned cavity ring-down spectroscopy technology: new insights and important caveats for deuterium excess measurements in tropical areas in comparison with isotope-ratio mass spectrometry, Rapid Commun. Mass Sp., 25, 3469–3480, 2011. 2824
Uemura, R., Matsui, Y., Yoshimura, K., Motoyama, H., and Yoshida, N.: Evidence of deuterium excess om water vapor as a indicator of ocean surface condition, J. Geophys. Res., 113, 9114, doi:10.1029/2008JD010209, 2008. 2823

Wang, L., Caylor, K. K., and Dragoni, D.: On the calibration of continuous, high-precision $\delta^{18}O$ and $\delta^{2}H$ measurements using an off-axis integrated cavity output spectrometer, Rapid Commun. Mass Sp., 23, 530–536, 2009. 2824

Yakir, D. and Wang, X. F.: Fluxes of CO_2 and water between terrestrial vegetation and the atmosphere estimated from isotope measurements, Nature, 380, 515–517, 1996. 2823

Table 1. δD and δ^{18}O values of water standards measured using the IRMS and the WVIA.

Sample	δD			δ^{18}O			N
	δ_{IRMS}	δ_{WVIA}	$\Delta\delta$	δ_{IRMS}	δ_{WVIA}	$\Delta\delta$	
Std 11	−0.1			0.08			
Std 6	−61.3	−62.4 ± 1.3	1.07	−8.65	−8.69 ± 0.23	0.04	15
Std 12	−86.4	−86.4 ± 0.7	0.04	−12.03	−11.93 ± 0.14	0.10	15
Std X1	−138.3	−138.5 ± 1.0	0.22	−18.36	−18.35 ± 0.16	0.02	20
Std 9	−189.2	−190.0 ± 0.7	0.80	−24.76	−24.69 ± 0.16	0.07	15
Std X2	−225.7	−226.3 ± 0.6	0.62	−29.45	−29.44 ± 0.15	0.01	20
Std 13	−257.7	−257.0 ± 1.4	0.68	−33.39	−33.22 ± 0.24	0.17	15
Std X3	−332.7	−331.1 ± 0.6	1.52	−42.44	−42.35 ± 0.17	0.09	20
Std 10	−397.9			−50.87			

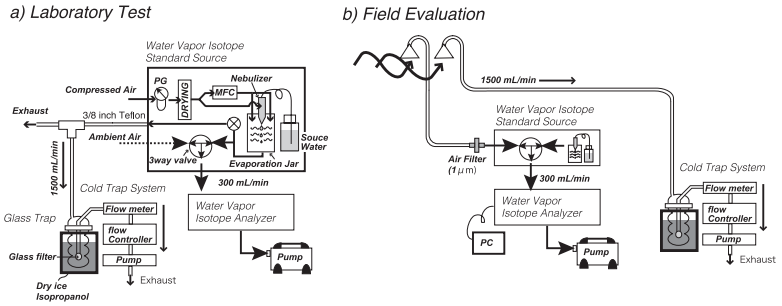

Fig. 1. Experimental setup for **(a)** laboratory test and **(b)** field evaluation.

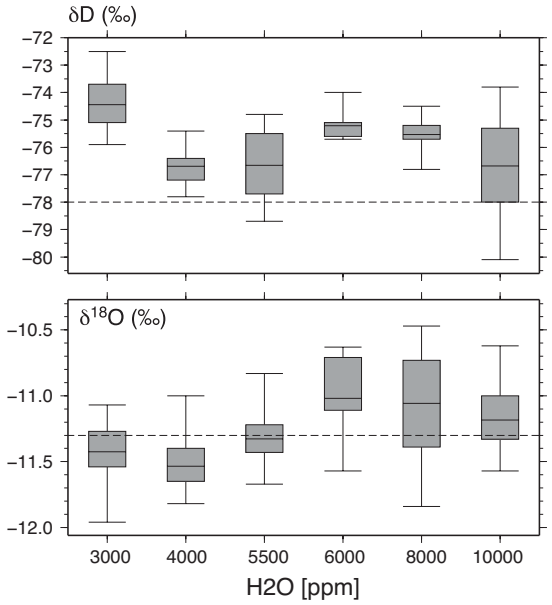

Fig. 2. Analytical variations in the δD and δ^{18}O of cold trapped vapor sampled from a WVISS exhaust line with different H_2O concentrations. Repeated analysis of standard water (δD = −78 ‰ and δ^{18}O = −11.3 ‰) was run at 6 levels of vapor concentration from 3000 to 10 000 ppm. The broken line represents known isotopic values determined via IRMS measurement. The box and whisker plots of δ^{18}O data represent the median (dark bar), 25–75 % quantile range (inter-quantile range [IQR] shown as the box), and maximum and minimum values (whiskers) for repeated experiments.

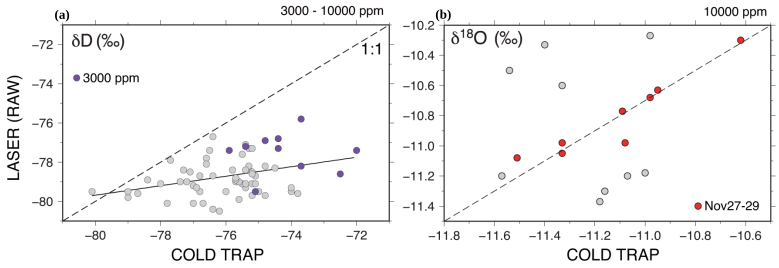

Fig. 3. A comparison of cold trap vapor analysis with direct vapor measurement using the WVIA: **(a)** δD in a concentration range of 3000–10 000 ppm; the purple points represent values at 3000 ppm; and **(b)** δ^{18}O at 10 000 ppm only; the red plots represent data from 27–29 November 2011. Broken lines represent the 1:1 relationship. These WVIA measurements are the uncorrected and uncalibrated δD and δ^{18}O values.

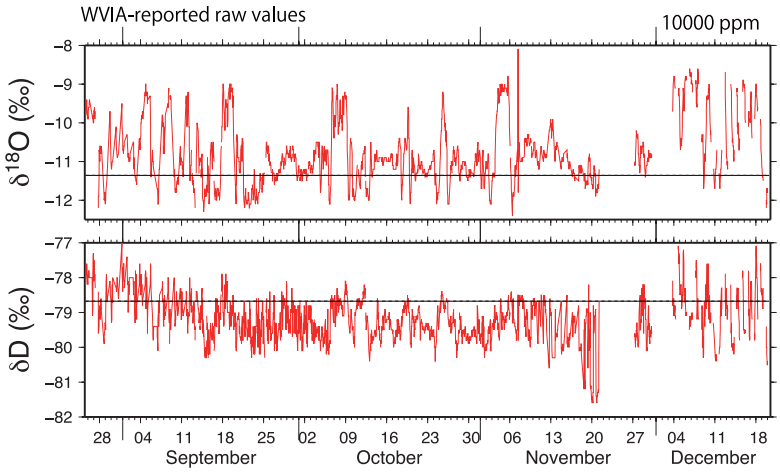

Fig. 4. Time series of uncalibrated δD and δ^{18}O values of a single water standard (δD = −78 ‰ and δ^{18}O = −11.3 ‰) measured using the WVIA from late August through mid-December, 2011. The data represent the uncorrected and uncalibrated δD and δ^{18}O values recorded by the WVIA and show the amount of instrument drift over the multimonth period.

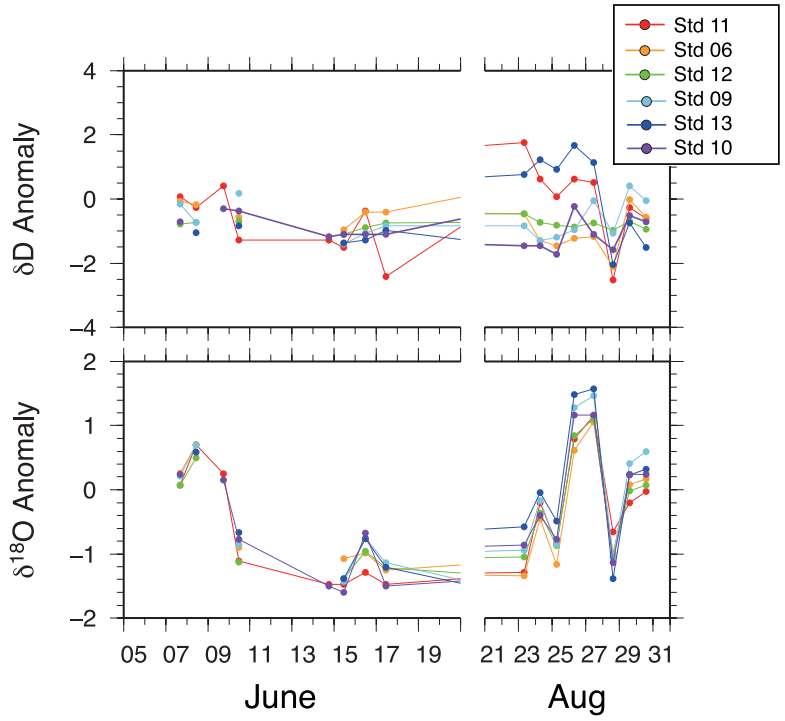

Fig. 5. Comparison of time-dependent δD and δ^{18}O variations of six water standards with different isotopic compositions. Plotted values are expressed as a normalized anomaly, that is, a departure from the long-term mean for the analysis period, divided from the standard deviation during this period.

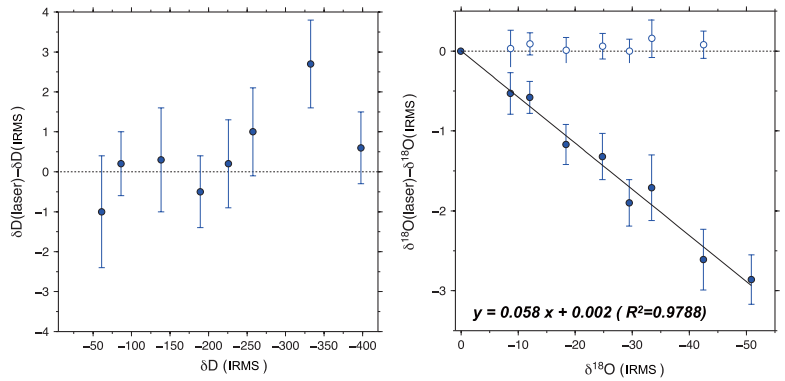

Fig. 6. The difference in WVISS based δD and δ^{18}O values from known IRMS based values of each water standard (blue circle). In both figures, the x-axis represents known IRMS based SMOW/SLAP scale values. For δ^{18}O, collected SMOW scale values are also plotted at the top of the figure (white circle).

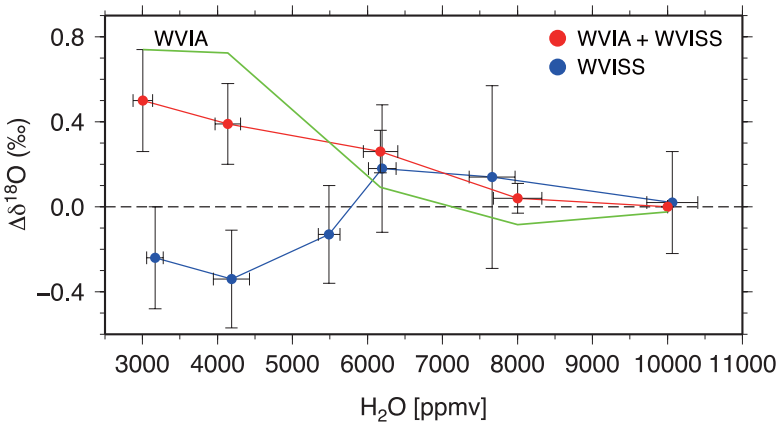

Fig. 7. δ^{18}O anomaly with changing water vapor concentrations. Anomalies are calculated by subtracting the mean value at 10 000 ppm from measured values at a given water vapor concentration. Error bars show the standard deviation of repeated experiments. The WVISS was run with different water vapor concentrations and the resultant vapor was measured with the WVIA (red line). To escape from the influence of WVIA temporal drift, this experiment was undertaken in a 30 min. Moisture from WVISS exhaust air was collected using the cold trap system and analyzed off line (blue). To collect a sufficient amount of water for isotope analysis, vapor trapping continued more than two hours. A large spread in the error bar at each vapor concentration may result from isotopic changes in WVISS-generated air and analytical error. Humidity bias stemming solely from the WVIA (green line) was calculated by subtracting the mean values of water vapor generated by the WVISS from WVIA-measured values at a given water vapor concentration.

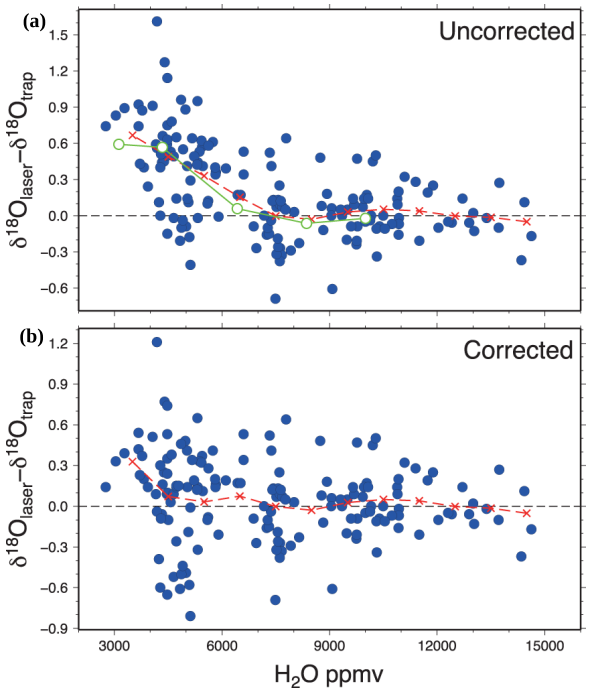

Fig. 8. The δ^{18}O difference in atmospheric water vapor between WVIA data and cold trap vapor samples as a function of changing water vapor concentrations. **(a)** WVIA data without a water vapor concentration correction and **(b)** corrected data. WVIA data was integrated during vapor trapping. The broken red line with crosses shows average values at each vapor concentration from 3500 ppm to 14 500 ppm. For comparison, the water concentration bias arising from WVIA and shown as a green line in Fig. 7 was superimposed in the uncorrected version.

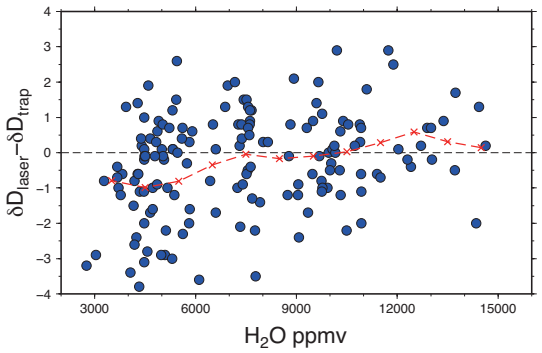

Fig. 9. The same as Fig. 8b, but for δD values.

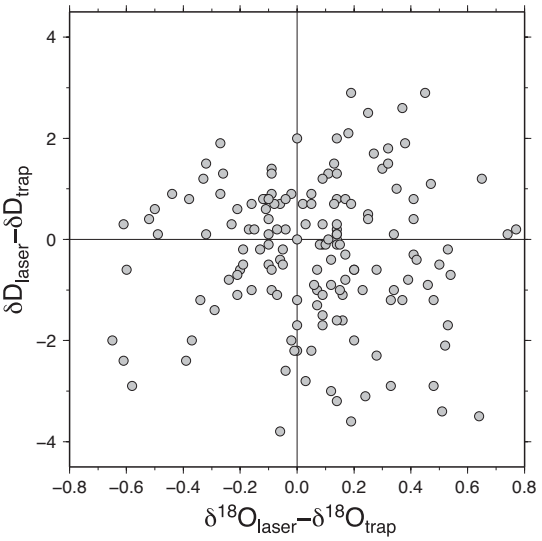

Fig. 10. Comparison of δD and δ^{18}O of water vapor collected via the cold trap method and directly measured using the WVIA. For improved comparison, the time-averaged isotopic values of WVIA measurements during vapor trapping periods are plotted.

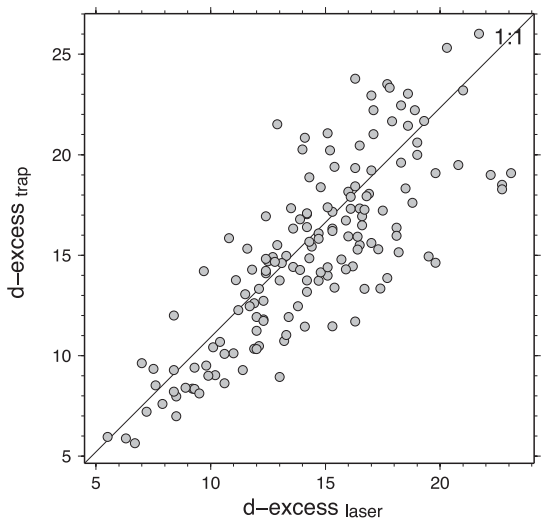

Fig. 11. Comparison of *d*-excess in water vapor using the cold trap and WVIA methods. The WVIA-measured *d*-excess values were derived from corrected and calibrated δD and δ^{18}O values and then time-averaged values were calculated.